Stroke

BASIC AND TRANSLATIONAL SCIENCES

Transcranial Cortex-Wide Imaging of Murine Ischemic Perfusion With Large-Field Multifocal Illumination Microscopy

Zhenyue Chen, PhD; Quanyu Zhou, PhD; Jeanne Droux, MS; Yu-Hang Liu, PhD; Chaim Glück, PhD; Irmak Gezginer, MS; Matthias Wyss, PhD; Hikari A.I. Yoshihara, PhD; Diana Rita Kindler, MS; Bruno Weber, PhD; Susanne Wegener, MD; Mohamad El Amki, PhD; Daniel Razansky, PhD

BACKGROUND: Ischemic stroke is a common cause of death worldwide and a main cause of morbidity. Presently, laser speckle contrast imaging, x-ray computed tomography, and magnetic resonance imaging are the mainstay for stroke diagnosis and therapeutic monitoring in preclinical studies. These modalities are often limited in terms of their ability to map brain perfusion with sufficient spatial and temporal resolution, thus calling for development of new brain perfusion techniques featuring rapid imaging speed, cost-effectiveness, and ease of use.

METHODS: We report on a new preclinical high-resolution angiography technique for murine ischemic stroke imaging based on large-field high-speed multifocal illumination fluorescence microscopy. We subsequently showcase the proposed method by monitoring therapeutic effects of thrombolysis in stroke (n=6), further performing cross-strain comparison of perfusion dynamics (n=6) and monitoring the therapeutic effects of sensory stimulation–based treatment (n=11).

RESULTS: Quantitative readings of hemodynamic and structural changes in cerebral vascular network and pial vessels were attained with 14.4-μm spatial resolution at 80-Hz frame rate fully transcranially. The in vivo perfusion maps accurately delineated the ischemic core and penumbra, further exhibiting a strong correlation (86.1±4.5%) with ex vivo triphenyl tetrazolium chloride staining, significantly higher than for the conventional laser speckle contrast imaging method. Monitoring of therapeutic effects of thrombolysis confirmed that early recanalization could effectively save the penumbra while reducing the infarct area. Cross-strain comparison of perfusion dynamics affirmed that C57BL/6 mice feature a larger penumbra and smaller infarct core as compared with BALB/c mice, which have few or no collaterals. Sensory stimulation–based treatment could effectively enhance blood flow and abolish perfusion deficits in the ischemic core and penumbra regions.

CONCLUSIONS: A high-speed fluorescence-based angiography method for transcranial stroke imaging in mice is introduced, which is capable of localizing brain perfusion changes and accurately assessing the ischemic penumbra. Compared with the whole-brain x-ray computed tomography and magnetic resonance imaging methods, which are conventionally used for stroke diagnosis and therapeutic monitoring, the new approach is simple and cost-effective, further offering high resolution and speed for in vivo studies. It thus opens new venues for brain perfusion research under various disease conditions such as stroke, neurodegeneration, or epileptic seizures.

GRAPHIC ABSTRACT: A graphic abstract is available for this article.

Key Words: angiography ■ cause of death ■ microscopy, fluorescence ■ perfusion imaging ■ stroke

Correspondence to: Mohamad El Amki, PhD, Department of Neurology, University Hospital and University of Zurich, Frauenklinikstrasse 26, 8091 Zurich, Switzerland, Email mohamad.elamki@usz.ch; or Daniel Razansky, PhD, Institute for Biomedical Engineering, University of Zurich and ETH Zurich, Wolfgang-Pauli-Strasse 27, 8093 Zurich, Switzerland, Email daniel.razansky@uzh.ch

Preprint posted on BioRxiv November 3, 2023. doi: https://doi.org/10.1101/2023.11.01.564959.
Supplemental Material is available at https://www.ahajournals.org/doi/suppl/10.1161/STROKEAHA.124.047996.
For Sources of Funding and Disclosures, see page 181.

Stroke is available at www.ahajournals.org/journal/str

Nonstandard Abbreviations and Acronyms

BFI	blood flow index
CBF	cerebral blood flow
LHMI	large-field high-speed multifocal illumination
LSCI	laser speckle contrast imaging
MCA	middle cerebral artery
MTT	mean transient time
ROI	region of interest
TTC	triphenyl tetrazolium chloride
TTP	time to peak

Acute ischemic stroke is the second cause of death and the first cause of morbidity worldwide.[1] Emerging evidence indicates that the best outcomes are achieved when recanalization therapy is performed as soon as possible after stroke onset. During this short period, known as the golden hour, rapid determination of both reversibly (penumbra) and irreversibly (core) injured tissue is paramount.[2] Without early recanalization, the penumbra becomes infarcted while late recanalization may increase the rate of intracerebral bleeding and mortality.[3] Hence, fast identification of the ischemic penumbra and its expansion over time is crucial for assessing treatment benefits for patients with stroke. However, precision techniques for imaging the penumbra and brain perfusion alterations are still lacking.

Small animal x-ray computed tomography and magnetic resonance imaging are the mainstay for stroke diagnosis and therapeutic monitoring in preclinical studies. Computed tomography has a proven track record for assessing acute ischemic stroke and ruling out hemorrhage, yet it uses ionizing radiation and suffers from inferior sensitivity and soft tissue contrast.[1] While magnetic resonance angiography and diffusion- and perfusion-weighted imaging can provide comprehensive multiparametric assessment of the brain parenchyma and circulation,[4] those diagnostic procedures are not widely and immediately accessible. Furthermore, preclinical computed tomography and magnetic resonance imaging are generally limited in their ability to map brain perfusion with sufficient spatial and temporal resolution.

Optical imaging techniques have been explored as an accessible and cost-effective alternative for stroke studies in rodents. Although ex vivo histological imaging of brain sections allows for detailed evaluation of stroke injury, including neuronal apoptosis, necrosis and death, this technique lacks dynamic temporal information, requiring postmortem indirect inferences.[5] Conventional in vivo widefield fluorescence imaging suffers from poor spatial resolution due to strong light scattering in the skull and brain tissue, making the assessment of perfusion and single vessel circulation unattainable. On the other hand, point scanning microscopy techniques, such as laser scanning confocal microscopy, optical coherence tomography, or multiphoton microscopy, can achieve superior spatial resolution but commonly involve highly invasive craniotomy procedures.[6] Those techniques further suffer from restricted field of view, making them unsuitable for monitoring the vascular structural change on a brain-wide scale. Optical microangiography based on the Michelson optical interferometer, similar to an optical fiber–based frequency domain optical coherence tomography, allowed for the assessment of 3-dimensional cerebrovascular pathophysiology at depths of ≈1.5 mm through intact skull yet suffered from a relatively poor temporal resolution of 50 s to finish 1 scan.[7] There is an increasing number of studies exploring the potential of near-infrared spectroscopy due to its relatively deep penetration and noninvasiveness.[8] Although near-infrared spectroscopy can partially map superficial cerebrovascular responses, its value for acute stroke imaging is greatly limited by poor spatial resolution and low specificity. Other optical imaging techniques such as time-resolved absolute quantification methods,[9] indocyanine green-based perfusion assessment,[10] and laser speckle contrast imaging (LSCI)[11] have been exploited in intraoperative applications. However, these techniques provide poor spatial resolution due to strong scattering or otherwise limited functional information in terms of blood flow and perfusion constant for assessing acute ischemic stroke.

In this work, we introduce a cortex-wide fluorescence-based angiography technique for murine ischemic stroke imaging of microvasculature, functional dynamics, and perfusion maps with high spatial and temporal resolution. We subsequently perform in vivo assessment of ischemic core and penumbra and monitoring of recanalization therapies, depicting the process of rescuing the penumbra via reperfusion by thrombolysis. The in vivo data are validated with corresponding triphenyl tetrazolium chloride (TTC) staining of brain infarctions. Furthermore, we performed cross-strain comparison of poststroke perfusion dynamics in mice with different vascular architectures (C57BL/6 and BALB/c), revealing different core and penumbra sizes and collateral recruitment patterns. Finally, we performed monitoring of sensory stimulation–based treatment for stroke with the proposed method to assess its therapeutic effects.

METHODS

All data relevant to this study are included in the article or uploaded as the Supplemental Material. Raw data and code that support the findings of this study are available from the corresponding authors upon request.

Animal Models

Six BALB/c mice (8- to 9-week-old; Charles Rivers) and 14 C57BL/6 mice (8- to 9-week-old; Charles Rivers) were

used in this work. Animals were housed in individually ventilated, temperature-controlled cages under a 12-hour dark/light cycle. Pelleted food (3437PXL15; CARGILL) and water were provided ad libitum. All experiments were performed in accordance with the Swiss Federal Act on Animal Protection and were approved by the Cantonal Veterinary Office Zurich (ZH165/2019). The usage of animals in each experiment was reported using the ARRIVE guidelines (Animal Research: Reporting of In Vivo Experiments).[12]

Thrombin Stroke Model

The thrombin stroke model was used as described previously.[13] In brief, mice were fixed in a stereotactic frame, the skin between the left eye and ear was incised, and the temporal muscle was retracted. A small hole was drilled in the temporal bone to access the middle cerebral artery (MCA) while the skull was kept intact. To induce the formation of a clot, 1 µL of purified human α-thrombin (1UI; HCT-0020; Haematologic Technologies, Inc) was injected into the MCA with a glass pipette. The pipette was removed 10 minutes after thrombin injection. Ischemia induction was considered stable when cerebral blood flow (CBF) rapidly dropped to at least 50% of baseline level in the MCA territory by checking the LSCI images.[13,14] Note that this threshold was chosen based on our previous experience. We calculated the poststroke CBF drop for all the mice used in our work and observed 74.2% drop in the mean perfusion values, agreeing well with the conventional thresholds defining stable ischemia induction.[15–17]

Stroke Treatment With tPA Administration

tPA (tissue-type plasminogen activator) treatment was performed 1 hour post-surgery after stroke screening with sequential large-field high-speed multifocal illumination (LHMI) and LSCI. Human tPA (0.9 mg/kg, Actilyse; Boehringer Ingelheim) was administrated through tail vein infusion with a syringe pump at a constant infusion speed of 6 µL/min. Other potential confounders were not controlled.

Sensory Stimulation–Based Treatment for Stroke

For stroke treatment with sensory stimulation, 11 C57BL/6 mice were separated into the intervention group (n=7) and the sham-controlled group (n=4). All mice were anesthetized with ketamine and xylazine, and somatosensory cortex of the hindlimb (S1HL) cortex region was first mapped using intrinsic signal optical imaging (see Note S1 for details on intrinsic signal optical imaging). Immediately after stroke, perfusion imaging with LSCI and LHMI was performed. Mice in the intervention group received electrical hindpaw stimulation for 100 s (pulse duration, 1 ms; repetition frequency, 4 Hz; pulse amplitude, 1 mA) with a time interval of 10 minutes and a duration of 1 hour. Mice in the control group did not receive any stimulation while all other factors (eg, air supply, heating, and physiological status monitoring) were kept the same as for the stimulated group. During the experiment, an oxygen/air mixture (0.2/0.8 L·min^{-1}) was provided through a breathing mask. The body temperature was kept around 37 °C with a feedback-controlled heating pad. Peripheral blood oxygen saturation, heart rate, and body temperature were monitored (PhysioSuite; Kent Scientific) in real time.

In Vivo Imaging

For in vivo imaging, the mice were anesthetized with isoflurane (3.0% v/v for induction and 1.5% v/v during experiments) in 20% O_2 and 80% air at a flow rate of ≈0.5 L/min. The scalp was removed to reduce light scattering. To obtain the cerebral vascular network and the perfusion pattern poststroke and pre-tPA treatment, each mouse was administrated the cyanine fluorescent dye (sulfo-cyanine-5.5-carboxylic acid; Lumiprobe GmbH, Germany; https://www.lumiprobe.com) solved in PBS (50 µL, 2 mg/mL) through a tail vein injection while recording with the LHMI system, followed by LSCI measurement (see Notes S2 and S3 for details on the imaging methods). Sulfo-Cyanine-5.5-carboxylic acid is a free, nonactivated carboxylic acid with a molecular mass of 1017.31 and shows good solubility in water, a large extinction coefficient (211 000/L·mol^{-1} cm^{-1}), high fluorescence quantum yield (0.21), and peak absorption at 673 nm,[18] making it an ideal contrast agent to assess perfusion dynamics in vivo. Stroke treatment with tPA administration was performed after the first round of in vivo stroke imaging (1 hour poststroke). After finishing the infusion, the mouse was kept in a small animal recovery chamber (Hugo Sachs Elektronik GmbH) for 30 minutes, followed by the second round of stroke imaging with both LHMI and LSCI as described above. For LHMI fluorescence microscopy, data were recorded right after fluorescence dye injection and lasted for 20 s. Each LHMI image was acquired through a 30×30 raster scan with the acousto-optic deflector at ≈11 µm step size, which corresponded to an effective frame rate of 80 Hz. For LSCI, data were recorded for 1 minute with an integration time of 250 ms for each LSCI image corresponding to a frame rate of 4 Hz.

Ex Vivo Validation of Lesion Size

To validate the in vivo measurement of the lesion size, mice were euthanized 24 hours after the experiment by receiving an overdose injection of pentobarbital (200 mg/kg IP) followed by decapitation. Brains were extracted and placed in 2% 2,3,5-TTC (catalog No. T8877; Sigma-Aldrich, St. Louis, MO) for 10 minutes at 37 °C to delineate infarcts that appear pale after staining. Ex vivo infarct areas were determined by setting a threshold of 0.5 to normalized TTC image. Specifically, pixels with intensities higher than the setting threshold were classified into infarct region. To estimate the accuracy of LHMI and LSCI measurements, the correlation coefficient between in vivo infarct core area and ex vivo infarct area was calculated for each mouse by $coefficient = S_{overlapped}/S_{TTC}$, where $S_{overlapped}$ is the overlapped area between LHMI/LSCI and TTC-stained infarct area and S_{TTC} is the TTC-stained infarct area.

Statistical Analysis

Twenty mice including 14 C57BL/6 mice and 6 BALB/c mice were used in this study. In each data set, core and penumbra regions were selected based on blood flow index (BFI) change map, followed by the computation for averaged fluorescence intensity, BFI, time to peak (TTP), LSCI intensity, and vessel fill fraction in the regions of interest (ROIs). Data were shown in box-and-whiskers plots with median indicated as the central line inside the boxes and interquartile range indicated as the box length. Maximum and minimum values were labeled with the whiskers. The correlation coefficients between LHMI/LSCI

Stroke. 2025;56:170–182. DOI: 10.1161/STROKEAHA.124.047996

and TTC staining passed Shapiro-Wilk normality test and were tested with paired *t* test (2-tailed) using the GraphPad software. A $P<0.05$ was considered statistically significant.

RESULTS

In Vivo Transcranial Fluorescence Microscopy Allows Noninvasive Cortex-Wide Perfusion Imaging in Ischemic Stroke

The LHMI technique capitalizes on the fast scanning based on an acousto-optic deflector and a beam-splitting grating to generate a uniform illumination grid of 17×17 foci (Figure 1A). By rapidly scanning the illumination grid and synchronizing data acquisition with a high-speed camera, a combination of a large field of view of 7×7 mm^2, high spatial resolution of 14.4 µm, and high frame rate of 80 Hz was achieved, thus exceeding imaging performance as compared with the originally reported implementation.[19] The complete experimental procedure included several steps. First, ischemic stroke is induced by injecting thrombin into the right MCA as described previously.[13,14] Subsequently, time-lapse LHMI images are acquired and compared with the images recorded with the well-established LSCI technique. For the LHMI imaging, fluorescence dye Sulfo-Cyanine5.5 (Sulfo-Cyanine-5.5-carboxylic acid) is administrated intravenously through the tail vein. For treated animals with thrombolysis, tPA (0.9 mg/kg) was administered as described previously[20] after LHMI imaging, that is, 60 minutes poststroke. For sensory stimulation treatment, hindpaw electrical stimulation was performed (Figure 1B).

An offline data processing pipeline was developed to facilitate stroke assessment (Figure 1C). LHMI images were first reconstructed and subsequently coregistered with the LSCI images. Pixel-wise TTP, BFI, and mean transient time (MTT) maps were calculated from the LHMI image stack. Principal component analysis was performed to the image stack to distinguish the skull vessels and brain vessels (arterial and venous vessels) based on their different perfusion profiles. Blood flow velocity and CBF were calculated based on ROIs in different vessels (see Figure S1 and Note S4 for more details on the calculations). Infarct core and penumbra regions were obtained after applying thresholds to the BFI signal changes by comparing the ipsilateral and contralateral hemispheres. Note that the cortical blood flow from the contralateral hemisphere remained unchanged from the baseline following the stroke surgery, as verified with fluorescence localization microscopy[21] (Figure S2; Note S5), which is also in line with previous reports.[22] ROIs including core and penumbra were selected to perform further statistical analysis on perfusion constants and vessel fill fraction. Finally, validation of the in vivo measurement was performed by TTC staining, which measures ischemic infarction in the isolated brains.

Mouse brains were imaged (n=3 C57BL/6 mice) with LHMI microscopy prestroke and poststroke onset to map the cerebral microcirculation. Principal component

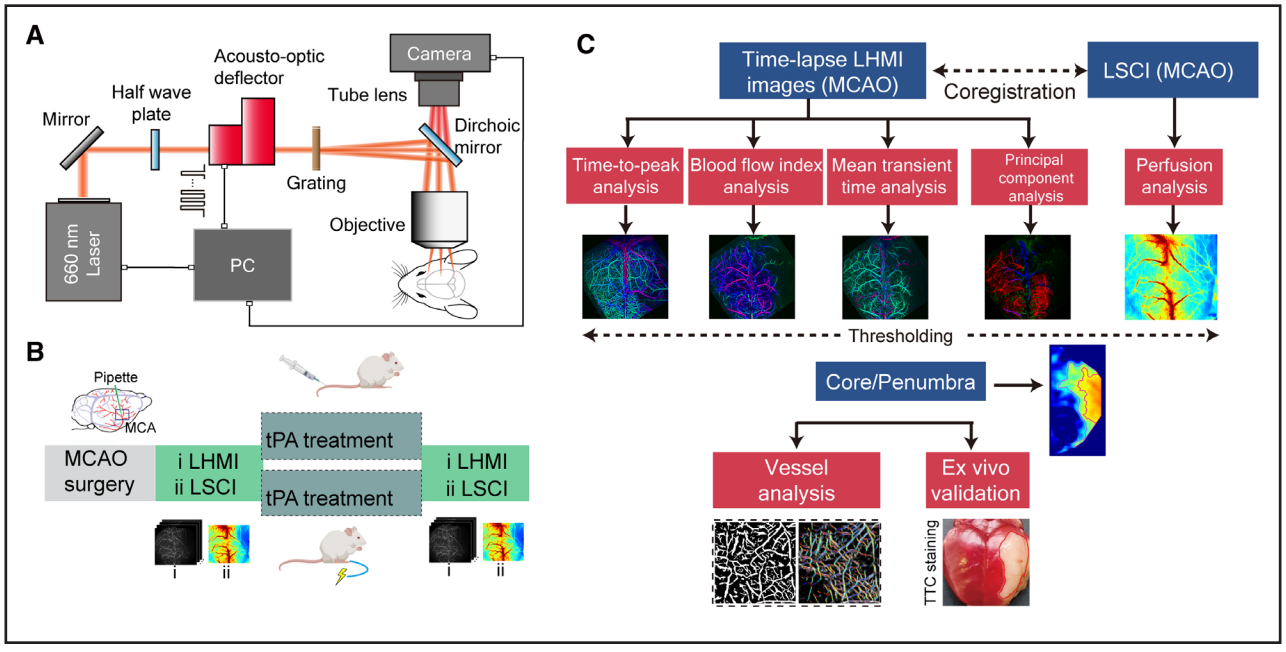

Figure 1. Stroke imaging system and methodology.
A, Layout of the large-field high-speed multifocal illumination (LHMI) fluorescence microscopy system. **B**, Experimental pipeline consisting of middle cerebral artery occlusion (MCAO) surgery and in vivo imaging pre-tPA (tissue-type plasminogen activator) and post-tPA treatment. **C**, Multiparametric characterization of stroke with LHMI in comparison to conventional laser speckle contrast imaging (LSCI) and ex vivo histology. MCA indicates middle cerebral artery; PC, personal computer; and TTC, triphenyl tetrazolium chloride.

analysis results before the stroke induction corroborated anatomic information (Figure 2A, left) on the cerebral vascular network and revealed clear perfusion differences between MCA, anterior cerebral arteries, and draining veins (Figure 2E).[23] Poststroke principal component analysis corroborated the occlusion of MCA while other vessels such as anterior cerebral arteries were not affected (Figure 2A, right). Notably, the accuracy of principal component analysis vessel classification may be compromised under pathological conditions, such as blood brain barrier leakage and abnormal blood flow caused by stroke or other vascular diseases. Due to the limited spatial resolution, vessels in the skull could not be accurately discerned from the brain vessel. BFI, MTT, and TTP maps in a representative data set showed clear perfusion deficit after stroke (Figure 2B through 2D). These results were further validated by independent measurement with LSCI, which showed similar patterns of perfusion deficits (Figure 2F).

We additionally investigated whether the brain perfusion readings provided by LHMI can be combined with neuronal calcium imaging to gain additional insights into the dynamics of the ischemic core and penumbra after stroke. For this, conventional widefield fluorescence imaging was performed in a Thy1-GCaMP6f mouse model prestroke and poststroke (30 minutes) at 40 frames/s (Note S6). Calcium signals were calculated between ROIs of different stroke regions and the contralateral side (Figure S3). Our data show an increased level of average amount of calcium and resting calcium in the penumbra, which could be due to massive hypometabolism in the neurons preventing

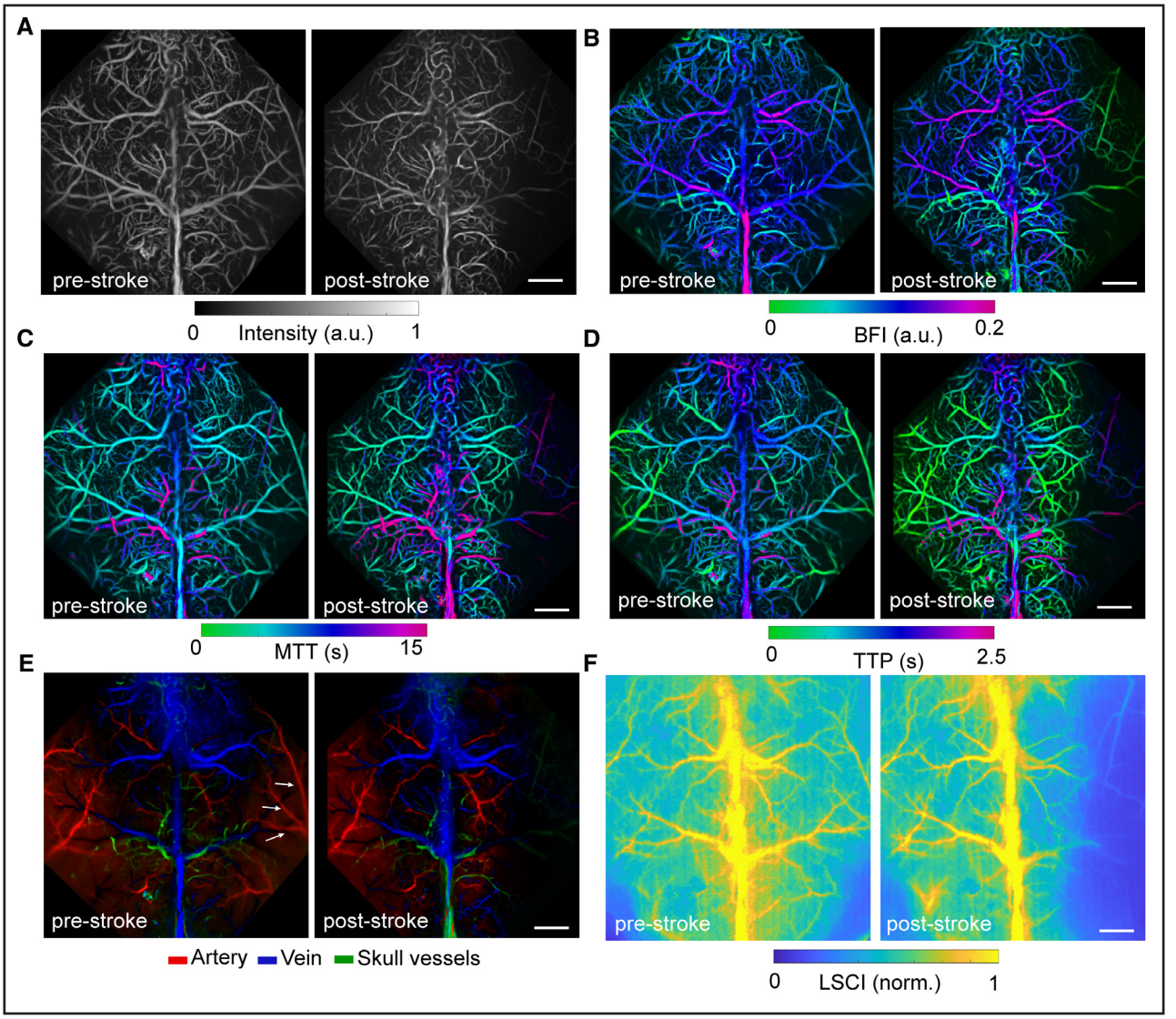

Figure 2. Transcranial large-field high-speed multifocal illumination fluorescence microscopy imaging allows detection of perfusion deficits in mouse stroke models.

A through **F**, Anatomic image, blood flow index (BFI), mean transient time (MTT), time to peak (TTP), principal component analysis results, and laser speckle contrast imaging (LSCI) from a representative mouse brain prestroke and poststroke. All scale bars=1 mm. The experiment was repeated independently in 3 mice (2 female and 1 male) with similar results. norm. indicates normalization.

calcium reuptake or extrusion. More interestingly, the calcium levels in the core were significantly decreased compared with the contralateral side, which may be attributed to neuronal death.

LHMI Fluorescence Microscopy Allows the Prediction of Therapy Success in Stroke

After the stroke induction, ischemic lesion boundary detection, including discrimination between the core of lesion and penumbra, could be accomplished with LHMI (Figure 3A and 3B). To demonstrate the precision of our proposed method, we further assessed the effect of a thrombolytic drug tPA, which allows CBF recovery and penumbra salvage. Mice were categorized into 2 different groups: stroke+tPA versus stroke controls (n=3 BALB/c male mice per group). Before treatment, fluorescence intensity, BFI, and fill fraction did not differ significantly between the 2 groups of mice. After tPA infusion, statistics on fluorescence intensity (Figure 3C), BFI (Figure 3D), LSCI (Figure S4A), lesion size estimation (Figure 3E), and vessel fill fraction (Figure S4B) clearly showed improved reperfusion both in the core and penumbra regions post-treatment. Interestingly, in the mice treated with tPA, TTC staining revealed the infarction area was highly correlated with the core region detected by LHMI, meaning the penumbra was saved (Figure 3B). Furthermore, in the control mice, TTC staining revealed a large infarct combining both core and penumbra detected by LHMI (Figure 3A). Compared with LSCI, correlation coefficients between the in vivo assessed core region and the TTC-stained infarct tissue reveal that LHMI has significantly higher diagnostic accuracy (mean±SD, 86.1±4.5% versus 75.4±5.2%; P=0.0032; Figure 3F). These data confirm the precision of LHMI microscopy in discriminating penumbra from the core.

LHMI Fluorescence Microscopy Reveals Strain-Related Perfusion Patterns Poststroke

Individual susceptibility to ischemic injury and the size of the ischemic penumbra vary greatly among different strains of mice due to the differences in their number of leptomeningeal collaterals. In this experiment, we aimed to perform LHMI in animals with different core/penumbra ratio. To do so, we induced stroke in mice with different collateral networks, namely, BALB/c having poor collaterals and C57BL/6 having rich collaterals (n=3 in each group). BFI, MTT, and TTP maps show clear differences between these 2 strains (Figure 4A versus Figure 4B; Figure S5). Specifically, BALB/c mice were more susceptible to the ischemic injury induced by stroke than C57BL/6 mice. Furthermore, BALB/c mice showed significantly reduced blood circulation in the infarct region with partially reduced blood flow (Figure 4C and 4D) and much shorter time latency (Figure 4E) than observed in the infarct region of C57BL/6 mice. Such discrepancy is congruent with previous reports and can be attributed to the lack of collateral vessels in BALB/c mice.[24]

The above observations are generally corroborated by the LSCI results (Figure 4A and 4B, second column). However, in comparison to LSCI, the core and penumbra regions inferred from the LHMI measurements (Figure 4A and 4B, third column) manifested significantly higher correlation with the TTC-stained brain tissue (Figure 4A and 4B, fourth column; Figure S6). This is arguably ascribed to the unspecific signal contrast mechanism of LSCI, which chiefly represents a nonlinear dependence between tissue scattering and blood flow velocity.[25] Note that TTP and MTT maps also manifest a clear boundary between the healthy and infarcted tissues. This is of importance since the infarcted areas have prolonged TTP and MTT values due to impaired microcirculation, which can serve as additional criteria for stroke assessment without requiring a priori information about blood circulation or comparison with the other brain hemisphere. Yet, TTP and MTT maps are inferior in distinguishing the infarct core and penumbra (Figures S7 through S9). Quantitative assessment of perfusion alterations was further performed in the infarct core and penumbra regions. Statistics on fluorescence signal intensity (Figure 4C) show that BALB/c mice exhibited reduced perfusion poststroke as compared with C57BL/6 mice while C57BL/6 mice had longer perfusion duration (Figure 4E). Consequently, BALB/c mice had larger infarct core size than C57BL/6 mice. Structural information analysis on vessel fill fraction (Figure 4F) also reveals that C57BL/6 mice had higher vessel perfusion rate at all sampling time instants as compared with BALB/c mice, which is consistent with aforementioned observations.

LHMI Fluorescence Microscopy Captures Dynamic Collateral Recruitment

To understand the impact of collaterals in maintaining brain perfusion after stroke, we compared the collateral circulation between C57BL/6 mice and BALB/c mice. Time-lapse images from a selected ROI covering both anterior cerebral artery and MCA were recorded from 1 representative mouse of each strain. Under baseline healthy conditions, collateral recruitment was not observed, suggesting that collateral flow was low (Figure 5A and 5B, first row). Following stroke induction, collateral flow became pronounced in C57BL/6 mice (Figure 5A, second row) but remained unapparent in BALB/c mice (Figure 5B, second row). Note that all the experimental parameters were kept the same for the assessment of both strains.

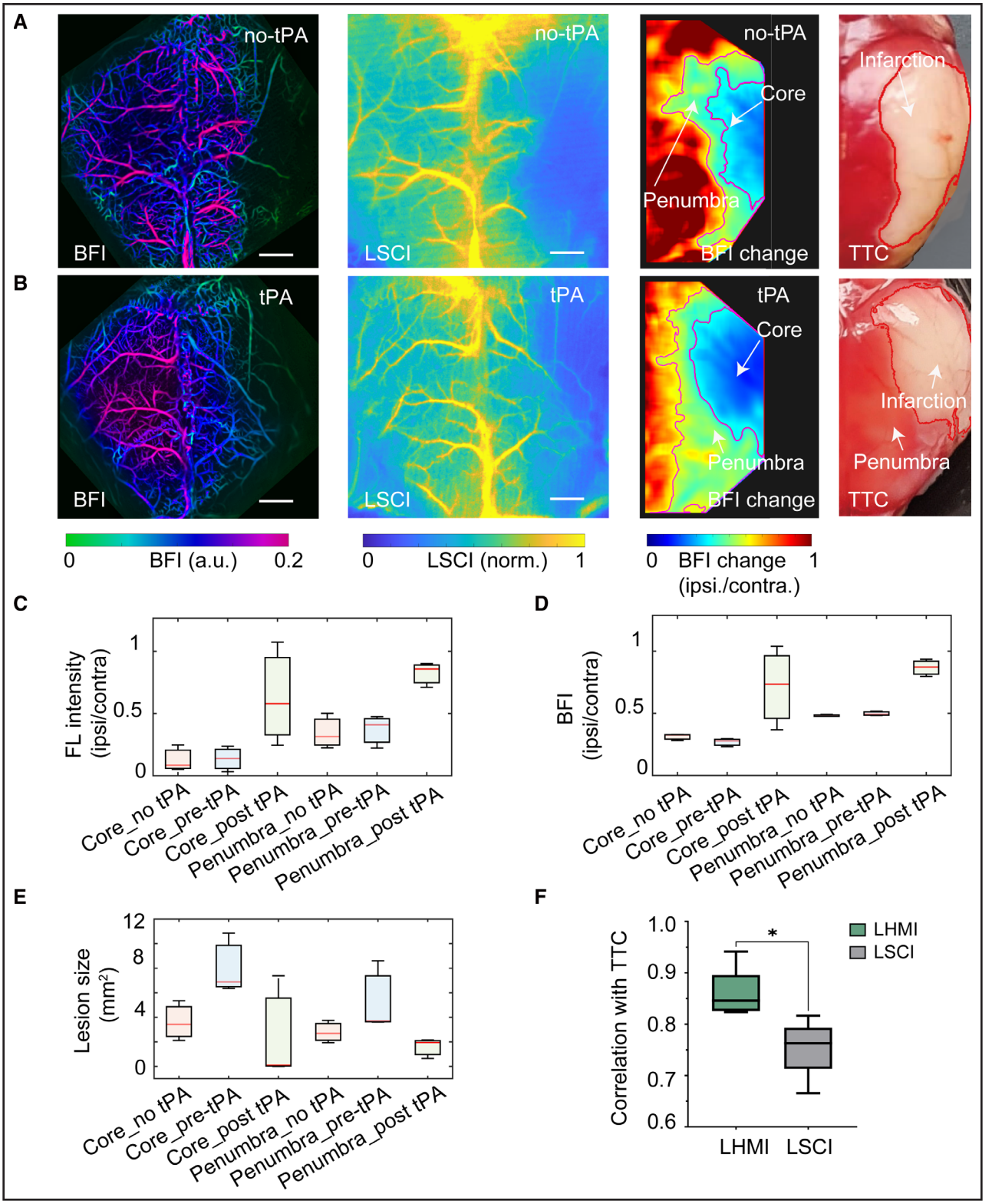

Figure 3. Stroke imaging results without tPA (tissue-type plasminogen activator) treatment in BALB/c mice.
A and **B**, Blood flow index (BFI), laser speckle contrast imaging (LSCI), BFI change, and corresponding triphenyl tetrazolium chloride (TTC) staining from the representative mouse without and with tPA treatment, respectively. **C** through **E**, Comparison between the large-field high-speed multifocal illumination (LHMI) fluorescence intensity, BFI, and lesion size for nontreated, pretreatment, and posttreatment mice. **F**, Infarct size correlation between in vivo measurement with LHMI/LSCI and TTC staining. Statistics performed with paired 2-tailed *t* test. All scale bars=1 mm. The experiment was repeated independently in 3 male mice per group with similar results. contra. indicates contralateral; FL, fluorescence; ipsi., ipsilateral; and norm., normalization.

 Stroke. 2025;56:170–182. DOI: 10.1161/STROKEAHA.124.047996

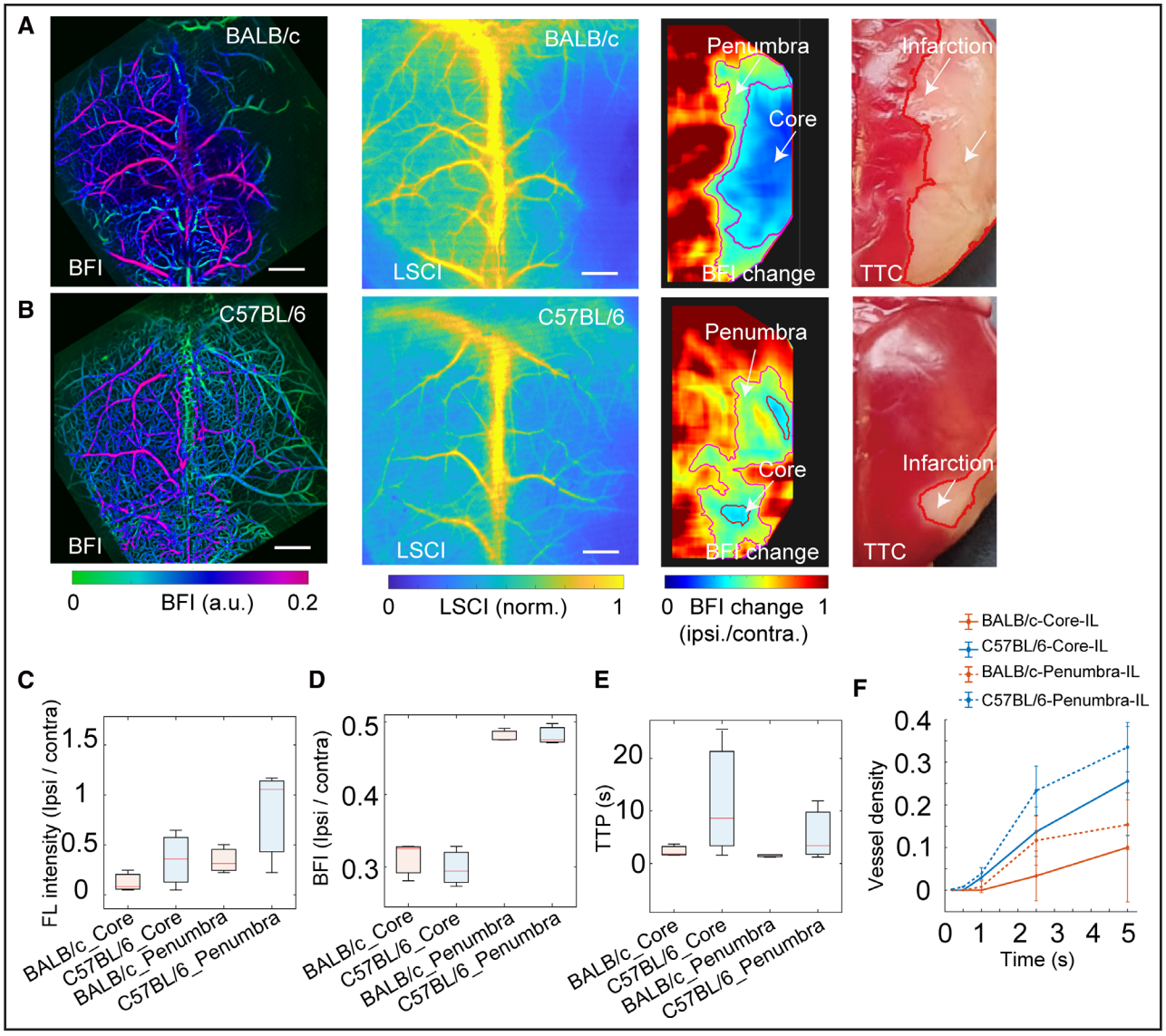

Figure 4. Experimental results on stroke imaging in BALB/c and C57BL/6 mice.
A and **B**, Blood flow index (BFI) and laser speckle contrast imaging (LSCI) images along with BFI signal change and triphenyl tetrazolium chloride (TTC) staining from representative BALB/c and C57BL/6 mice. **C** through **E**, Statistics on fluorescence intensity, BFI, and time to peak (TTP) from both BALB/c and C57BL/6 mice. All the parameters were normalized to values from the contralateral side. **F**, Vessel fill fraction time course in the core and penumbra regions from both BALB/c and C57BL/6 mice. All scale bars=1 mm. The experiment was repeated independently in 3 mice per group with similar results. There were 1 male and 2 female mice in the C57BL/6 group and 1 female and 2 male mice in the BALB/c group. contra. indicates contralateral; FL, fluorescence; ipsi., ipsilateral; and norm., normalization.

Sensory Stimulations, Delivered Within 1 Hour of Stroke Onset, Protect the Cortex From Perfusion Deficits

We finally investigated whether a sensory stimulation–based treatment can be exploited to improve cortical reperfusion after stroke. To this end, a sensory stimulation trial was performed immediately after the stroke onset (Figure 6A). The same experimental procedure was followed for animals from both the intervention (n=7) and the control (n=4) groups (see more details in Methods). Before inducing stroke, cortical activity and blood flow in the S1HL cortical region were assessed with intrinsic signal optical imaging and LSCI, respectively, while brain perfusion was measured with LHMI. To test the effect of sensory stimulation on poststroke brain perfusion, LHMI and LSCI were repeated immediately after stroke (0 hours) and at the end of the sensory stimulation–based treatment (1 hour poststroke).

BFI and LSCI (Figure 6B) displayed decreased hypoperfused area in the stimulated mice; however, the brain perfusion deficit was not different between the 0- and 1-hour poststroke time points in the nonstimulated mice (Figure 6C). Note that the perception of the lesion size from BFI map may be affected by the display of the image after contrast adjustment. Instead, ameliorating

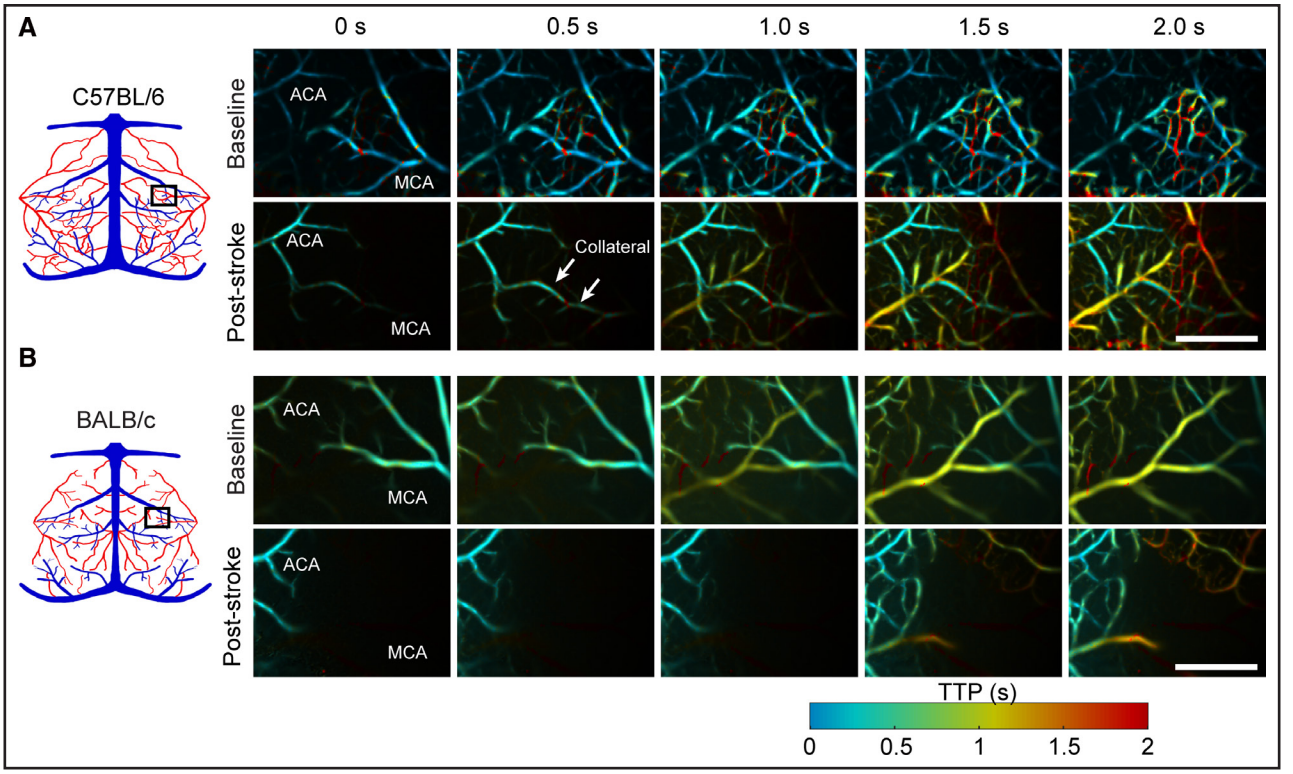

Figure 5. Dissimilar perfusion dynamics in C57BL/6 and BALB/c mice.
A, Representative time-lapse images post-fluorescence dye injection into 1 female C57BL/6 mouse. **Top** row, baseline before stroke. **Bottom** row, after stroke. **Left**, Imaged region of interest (ROI). **B**, Representative time-lapse images post-fluorescence dye injection into 1 male BALB/c mouse. **Top** row, baseline before stroke. **Bottom** row, after stroke. **Left**, Imaged ROI. All scale bars=1 mm. The experiment was repeated independently in 3 mice per group with similar results. There were 1 male and 2 female mice in the C57BL/6 group and 1 female and 2 male mice in the BALB/c group. ACA indicates anterior cerebral artery; MCA, middle cerebral artery; and TTP, time to peak.

brain perfusion was evident when evaluating the BFI changes. In contrast, the perfusion deficit has intensified at 1 hour poststroke for control mice by evaluating the BFI changes (Figure 6C). Statistics on the lesion size and its relative deviation from the intervention group (Figure 6D) show a clear contraction of the core region (P=0.0247) and a tendency for size reduction in the penumbra (P=0.2295) while the lesion sizes of both core and penumbra remained nearly unaltered in the control group (Figure 6E).

DISCUSSION

In ischemic stroke, both vascular morphology and blood flow information are crucial for accurately discerning the infarct core and penumbra. LHMI imaging brings major advantages for the detection and quantification of the structural and functional alterations after stroke, as well as for precise assessment of the core and penumbra regions. The method attains a powerful combination of high spatial resolution, millisecond temporal resolution, transcranial imaging capacity, and whole-cortex coverage. It is observed that blood flow in the infarct core is impaired to a greater extent as compared with the penumbra. Interestingly, the technique has been used to predict the success of thrombolytic therapy and a sensory stimulation–based treatment. Furthermore, our study shows how LHMI can be used to quantify differences in brain perfusion dynamics between mice with different stroke severities. Collateral recruitment, serving as an alternative blood supply to the infarct region, is of great interest in stroke as it crucially determines infarct severity, treatment efficacy, and recovery. In this work, by real-time monitoring of cortex-wide microcirculation, collateral recruitment was observed in C57BL/6 mice poststroke while no similar phenomenon was seen in the baseline (prestroke) measurements or in BALB/c mice.

In preclinical stroke research, LSCI has been widely adopted to provide brain-wide microcirculation mapping in real time and can indicate abnormal blood flow in different brain regions. However, the spatial resolution of LSCI is insufficient for accurately determining alterations in specific vessels. Furthermore, the overall ability of LSCI to provide quantitative readings of absolute blood flow, velocity, or tissue perfusion remains questionable.[26] Unlike LSCI whose imaging contrast mainly stems from scattering and is indirectly related to blood flow, the LHMI approach can image the blood flow directly, thus ensuring a higher interpretation power of the results and providing a higher correlation to the TTC staining.

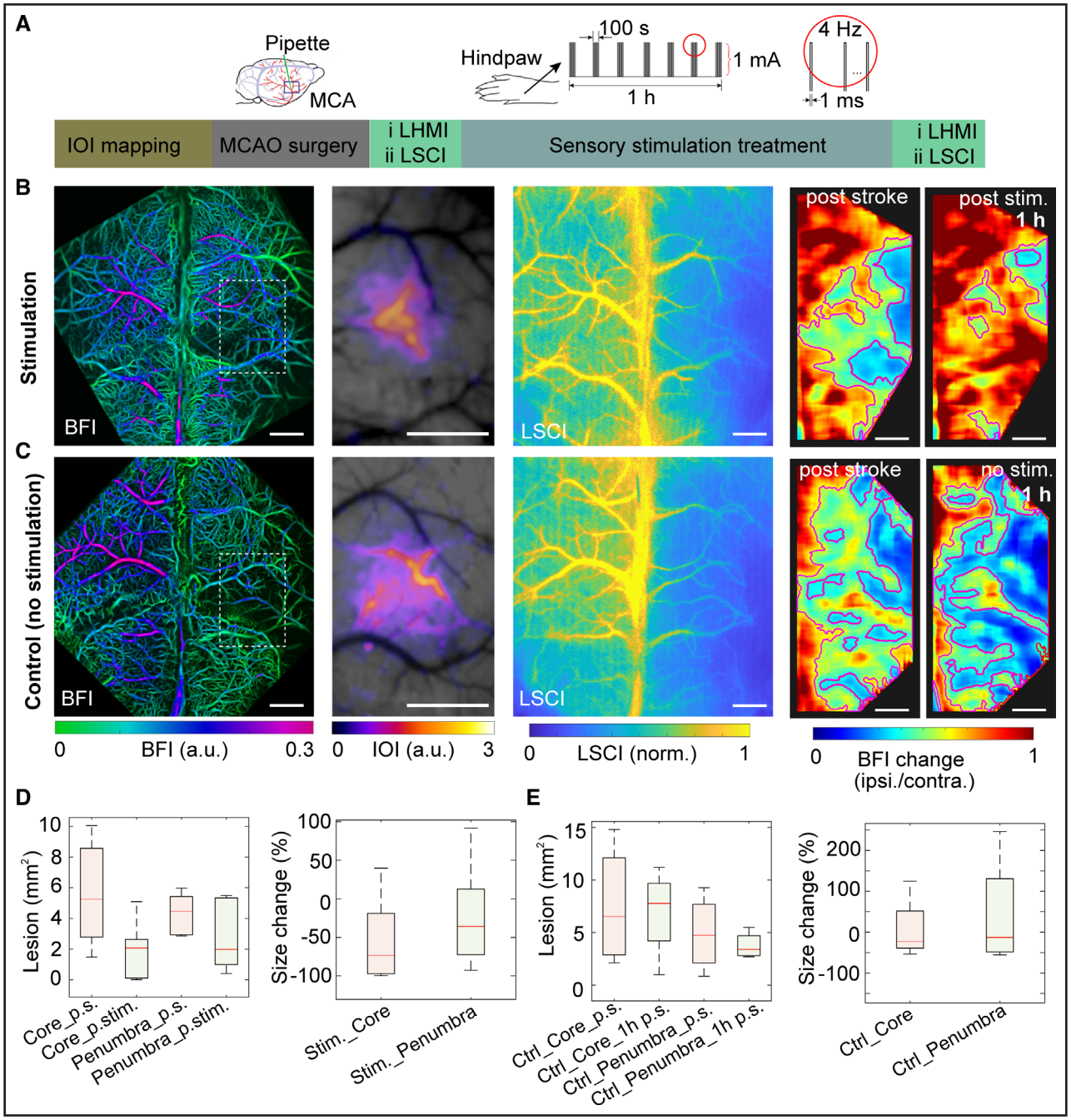

Figure 6. Effects of sensory stimulation treatment poststroke in C57BL/6 mice.
A, The experimental pipeline. **B**, Imaging results from 1 representative mouse with hindpaw stimulation. From **left** to **right**: blood flow index (BFI) post-stimulation, intrinsic signal (IOI) mapping of the stimulated S1HL region, laser speckle contrast imaging (LSCI) post-stimulation, BFI change poststroke and post-stimulation. **C**, Corresponding results from a representative control mouse post-stimulation. **D**, Core and penumbra size and their relative changes poststroke and post-stimulation. **E**, Core and penumbra size and their relative changes poststroke in control mice. All scale bars=1 mm. The experiment was repeated independently in 7 mice for sensory stimulation treatment (4 male and 3 female mice) and 4 mice (1 male and 3 female mice) for control with similar results. contra. indicates contralateral; ipsi., ipsilateral; LHMI, large-field high-speed multifocal illumination; MCA, middle cerebral artery; MCAO, middle cerebral artery occlusion; norm., normalization; and S1HL, somatosensory cortex of the hindlimb.

The ischemic penumbra has been in the center of stroke research for the last 40 years. The success for stroke therapy, including mechanical thrombectomy or intravenous thrombolysis, is based on a careful selection of patients who had salvageable penumbra. Therefore, stroke assessment studies might greatly benefit from a rapid and accurate tool for quantification of the ischemic penumbra. Despite major improvements in imaging methodology and instrumentation, it is widely accepted that the discrimination between penumbra and core regions is challenging with the existing imaging approaches. This is chiefly due to the considerable variability of

CBF thresholds used for delineating these regions. For instance, the classical penumbra has been defined as a region of 20% to 40% of residual CBF.[27] However, other studies defined the penumbra as a region with 30% to 50% CBF decrease[28,29] while some studies even considered regions with blood flow up to 60% to 70% as the penumbra region.[30,31] In this work, BFI residuals of <40% and 40% to 60% were considered for delineating the core and penumbra regions, respectively.

As an alternative to this hemodynamic concept, additional studies defined the penumbra as the tissue doomed to infarction in the absence of early reperfusion. Our data confirm that the penumbra detected with LHMI can be saved from tissue necrosis with reperfusion, otherwise it turns necrotic over time and merges into the infarct core. Several clinical trials have demonstrated the clinical benefits of salvaging the penumbra in patients with stroke,[32,33] underscoring the importance of imaging tools capable of predicting patient's response to thrombolytic treatments. It has also been shown that patients with a favorable imaging-based profile have strong collaterals and moderate infarct progression.[34] The size of core and penumbra is underpinned by the collateral supply to the tissue. In line with these clinical data, we have shown that LHMI can accurately predict the differences between infarcted areas in animals with rich and poor collaterals within the first minute after occlusion. Importantly, since our imaging system allows for transcranial imaging across the entire cortex, it was possible to perform multiparametric characterization of the pial vessels including perfusion dynamics and collateral recruitment. Clinically, this information will aid in monitoring the role of pial collaterals in infarct development and recovery. Note that the effective imaging depth of LHMI is limited by the ability to maintain a focused beam pattern as it propagates through turbid brain tissues, which typically corresponds to 0.5 to 1 mm usable depth range depending on the wavelength selection. The penetration depth can potentially be improved by performing imaging in the second near-infrared spectral window (NIR-II window, 1000–1700 nm), which benefits from reduced scattering, absorption, and negligible autofluorescence.[35] To obtain quantitative blood flow information along depth, LHMI can be combined with Doppler (or dynamic light scattering) optical coherence tomography owing to their compatibility as optical modalities.[36,37]

Given that evoked neuronal activity from paw stimulation is linked to an increase in blood flow, we further tested whether a potential treatment approach based on sensory stimulation may enhance brain perfusion, thus eliminating reperfusion deficits in the core and penumbra regions. It has been shown that sensory stimulation reduces the infarcted region both in the core and penumbra. Enhancing brain reperfusion with sensory stimulation is a particularly promising strategy for stroke treatment because it is noninvasive, nonpharmacological, and rapid, and has no side effects. Peripheral sensory stimulation during the hyperacute phase of stroke was reported to significantly recover neural activity.[38] Likewise, sphenopalatine ganglion stimulation has been shown likely to improve the functional outcome of patients with acute ischemic stroke clinically.[39] However, discrepancies in therapeutic effects have been reported. Contrarily to the positive results observed in rats, no differences were observed in mice with the same treatment between treated and untreated groups,[40] indicating a complex mechanism in stroke treatment using sensory stimulation. Indeed, a previous study revealed that when the activated cortex is within a critical range of ischemia, somatosensory activation of peri-infarct cortex may aggravate the situation by increasing the supply-demand mismatch and triggering peri-infarct depolarizations.[41] In the current study, the S1HL region was carefully selected such that it is able to redirect blood flow from anterior cerebral artery to MCA, yet located far enough from the peri-infarct region. The stroke treatments with sensory stimulation were accordingly only performed with mice having rich collateral vascularization.

To better understand the relationship between ischemic stroke and neuronal activities in the core and penumbra, the proposed method could potentially be combined with widefield fluorescence calcium imaging approaches using transgenic mouse lines like the Thy1GCaMP6f. However, it is important to recognize that it is not possible to identify unitary neuronal calcium activity with this approach but rather averaged neuronal resting calcium dynamics, which can be affected by multiple confounding factors. In general, the links between neuronal activity, calcium changes, and neuronal electric signals after stroke remain highly disputable and require further investigations.[42,43]

In summary, we present a high-speed fluorescence-based angiography for transcranial stroke imaging in mice that allows to (1) confirm ischemic stroke diagnosis, (2) localize the site of vascular occlusion, (3) detect hemodynamic changes and perfusion deficits, and (4) identify ischemic core and penumbra with high sensitivity and accuracy. The method is unique in its ability to localize brain perfusion changes and accurately assess the ischemic penumbra. LHMI can directly render images of diverse mouse models with local CBF variations. Overall, LHMI is simple and cost-effective compared with computed tomography/magnetic resonance imaging and may be used to improve our understanding of vascular responses under pathological conditions, ultimately facilitating clinical diagnosis, monitoring, and development of therapeutic interventions for cerebrovascular diseases.

ARTICLE INFORMATION

Received April 3, 2024; final revision received October 20, 2024; accepted November 7, 2024.

Affiliations

Institute of Pharmacology and Toxicology, Faculty of Medicine, University of Zurich, Switzerland (Z.C., Q.Z., Y.-H.L., C.G., I.G., M.W., H.A.I.Y., D.R.K., B.W., D.R.). Department of Information Technology and Electrical Engineering, Institute for Biomedical Engineering, ETH Zurich, Switzerland (Z.C., Q.Z., Y.-H.L., I.G., H.A.I.Y., D.R.K., D.R.). Institute of Precision Optical Engineering, School of Physics Science and Engineering, Tongji University, Shanghai, China (Z.C.). Department of Neurology, University Hospital and University of Zurich, Switzerland (J.D., S.W., M.E.A.). Zurich Neuroscience Center, Switzerland (J.D., C.G., M.W., B.W., S.W., M.E.A., D.R.).

Acknowledgments

Dr Chen conceived the study; Dr Chen, Dr Zhou, J. Droux, Dr Glück, and Dr El Amki performed the in vivo experiments; Dr Chen, I. Gezginer, D.R. Kindler, and Dr Yoshihara performed the magnetic resonance imaging validation experiments; J. Droux performed the triphenyl tetrazolium chloride staining; Dr Wyss performed the intrinsic signal optical imaging mapping; Drs Chen, Zhou, and Liu analyzed the data; Drs Chen, Zhou, and El Amki interpreted the results; Drs Chen and Razansky wrote the paper; Drs Weber, Wegener, El Amki, and Razansky supervised the project; all authors contributed constructively to the manuscript.

Sources of Funding

This study received grant support from the Betty and David Koetser Foundation; Hartmann Müller-Stiftung für Medizinische Forschung; the Swiss Heart Foundation; the Swiss National Science Foundation grants 310030_182703, 310030_200703 (SW), and 310030_192757 (DR); the US National Institutes of Health grant RF1-NS126102-01 (DR); and the UZH Clinical Research Priority Program (CRPP) stroke (SW).

Disclosures

None.

Supplemental Material

Figures S1–S9
Notes S1–S6

REFERENCES

1. Smith AG, Rowland HC. Imaging assessment of acute ischaemic stroke: a review of radiological methods. *Br J Radiol*. 2018;91:20170573. doi: 10.1259/bjr.20170573
2. Jovin TG, Chamorro A, Cobo E, de Miquel MA, Molina CA, Rovira A, San Román L, Serena J, Abilleira S, Ribó M, et al. Thrombectomy within 8 hours after symptom onset in ischemic stroke. *N Engl J Med*. 2015;372:2296–2306. doi: 10.1056/NEJMoa1503780
3. Molina CA, Montaner J, Abilleira S, Ibarra B, Romero F, Arenillas JF, Alvarez-Sabín J. Timing of spontaneous recanalization and risk of hemorrhagic transformation in acute cardioembolic stroke. *Stroke*. 2001;32:1079–1084. doi: 10.1161/01.str.32.5.1079
4. Kim BJ, Kang HG, Kim HJ, Ahn SH, Kim NY, Warach S, Kang DW. Magnetic resonance imaging in acute ischemic stroke treatment. *J Stroke*. 2014;16:131–145. doi: 10.5853/jos.2014.16.3.131
5. Zille M, Farr TD, Przesdzing I, Müller J, Sommer C, Dirnagl U, Wunder A. Visualizing cell death in experimental focal cerebral ischemia: promises, problems, and perspectives. *J Cereb Blood Flow Metab*. 2012;32:213–231. doi: 10.1038/jcbfm.2011.150
6. Akamatsu Y, Nishijima Y, Lee CC, Yang SY, Shi L, An L, Wang RK, Tominaga T, Liu J. Impaired leptomeningeal collateral flow contributes to the poor outcome following experimental stroke in the type 2 diabetic mice. *J Neurosci*. 2015;35:3851–3864. doi: 10.1523/JNEUROSCI.3838-14.2015
7. Li Y, Choi WJ, Wei W, Song S, Zhang Q, Liu J, Wang RK. Aging-associated changes in cerebral vasculature and blood flow as determined by quantitative optical coherence tomography angiography. *Neurobiol Aging*. 2018;70:148–159. doi: 10.1016/j.neurobiolaging.2018.06.017
8. Yang M, Yang Z, Yuan T, Feng W, Wang P. A systemic review of functional near-infrared spectroscopy for stroke: current application and future directions. *Front Neurol*. 2019;10:58. doi: 10.3389/fneur.2019.00058
9. Yokose N, Sakatani K, Murata Y, Awano T, Igarashi T, Nakamura S, Hoshino T, Katayama Y. Bedside monitoring of cerebral blood oxygenation and hemodynamics after aneurysmal subarachnoid hemorrhage by quantitative time-resolved near-infrared spectroscopy. *World Neurosurg*. 2010;73:508–513. doi: 10.1016/j.wneu.2010.02.061
10. Nakagawa I, Park HS, Yokoyama S, Yamada S, Motoyama Y, Park YS, Wada T, Kichikawa K, Nakase H. Indocyanine green kinetics with near-infrared spectroscopy predicts cerebral hyperperfusion syndrome after carotid artery stenting. *PLoS One*. 2017;12:e0180684. doi: 10.1371/journal.pone.0180684
11. Wang J, Lin X, Mu Z, Shen F, Zhang L, Xie Q, Tang Y, Wang Y, Zhang Z, Yang GY. Rapamycin increases collateral circulation in rodent brain after focal ischemia as detected by multiple modality dynamic imaging. *Theranostics*. 2019;9:4923–4934. doi: 10.7150/thno.32676
12. Kilkenny C, Browne WJ, Cuthill IC, Emerson M, Altman DG. Improving bioscience research reporting: the ARRIVE guidelines for reporting animal research. *PLoS Biol*. 2010;8:e1000412. doi: 10.1371/journal.pbio.1000412
13. El Amki M, Glück C, Binder N, Middleham W, Wyss MT, Weiss T, Meister H, Luft A, Weller M, Weber B, et al. Neutrophils obstructing brain capillaries are a major cause of no-reflow in ischemic stroke. *Cell Rep*. 2020;33:108260. doi: 10.1016/j.celrep.2020.108260
14. El Amki M, Lerouet D, Garraud M, Teng F, Beray-Berthat V, Coqueran B, Barsacq B, Abbou C, Palmier B, Marchand-Leroux C, et al. Improved reperfusion and vasculoprotection by the poly(ADP-ribose)polymerase inhibitor PJ34 after stroke and thrombolysis in mice. *Mol Neurobiol*. 2018;55:9156–9168. doi: 10.1007/s12035-018-1063-3
15. Bodhankar S, Chen Y, Vandenbark AA, Murphy SJ, Offner H. PD-L1 enhances CNS inflammation and infarct volume following experimental stroke in mice in opposition to PD-1. *J Neuroinflammation*. 2013;10:878.
16. Fujioka M, Hayakawa K, Mishima K, Kunizawa A, Irie K, Higuchi S, Nakano T, Muroi C, Fukushima H, Sugimoto M, et al. Adamts13 gene deletion aggravates ischemic brain damage: a possible neuroprotective role of adamts13 by ameliorating postischemic hypoperfusion. *Blood*. 2010;115:1650–1653. doi: 10.1182/blood-2009-06-230110
17. Binder NF, El Amki M, Glück C, Middleham W, Reuss AM, Bertolo A, Thurner P, Deffieux T, Lambride C, Epp R, et al. Leptomeningeal collaterals regulate reperfusion in ischemic stroke and rescue the brain from futile recanalization. *Neuron*. 2024;112:1456–1472.e6. doi: 10.1016/j.neuron.2024.01.031
18. Lumiprobe. www.lumiprobe.com/p/sulfo-cy55-carboxylic-acid
19. Chen Z, Mc Larney B, Rebling J, Deán-Ben XL, Zhou Q, Gottschalk S, Razansky D. High-speed large-field multifocal illumination fluorescence microscopy. *Laser Photon Rev*. 2019;14:1900070.
20. El Amki M, Lerouet D, Coqueran B, Curis E, Orset C, Vivien D, Plotkine M, Marchand-Leroux C, Margaill I. Experimental modeling of recombinant tissue plasminogen activator effects after ischemic stroke. *Exp Neurol*. 2012;238:138–144. doi: 10.1016/j.expneurol.2012.08.005
21. Chen Z, Zhou Q, Robin J, Razansky D. Widefield fluorescence localization microscopy for transcranial imaging of cortical perfusion with capillary resolution. *Opt Lett*. 2020;45:3470–3473. doi: 10.1364/OL.396123
22. Biose IJ, Dewar D, Macrae IM, McCabe C. Impact of stroke co-morbidities on cortical collateral flow following ischaemic stroke. *J Cereb Blood Flow Metab*. 2020;40:978–990. doi: 10.1177/0271678X19858532
23. Xiong B, Li A, Lou Y, Chen S, Long B, Peng J, Yang Z, Xu T, Yang X, Li X, et al. Precise cerebral vascular atlas in stereotaxic coordinates of whole mouse brain. *Front Neuroanat*. 2017;11:128. doi: 10.3389/fnana.2017.00128
24. Kanoke A, Akamatsu Y, Nishijima Y, To E, Lee CC, Li Y, Wang RK, Tominaga T, Liu J. The impact of native leptomeningeal collateralization on rapid blood flow recruitment following ischemic stroke. *J Cereb Blood flow Metab*. 2020;40:2165–2178. doi: 10.1177/0271678X20941265
25. Briers JD, Webster S. Laser speckle contrast analysis (LASCA): a nonscanning, full-field technique for monitoring capillary blood flow. *J Biomed Opt*. 1996;1:174–179. doi: 10.1117/12.231359
26. Duncan DD, Kirkpatrick SJ. Can laser speckle flowmetry be made a quantitative tool? *J Opt Soc Am A*. 2008;25:2088–2094. doi: 10.1364/josaa.25.002088
27. Paschen W, Mies G, Hossmann KA. Threshold relationship between cerebral blood flow, glucose utilization, and energy metabolites during development of stroke in gerbils. *Exp Neurol*. 1992;117:325–333. doi: 10.1016/0014-4886(92)90142-d
28. Bo B, Li Y, Li W, Wang Y, Tong S. Optogenetic translocation of protons out of penumbral neurons is protective in a rodent model of focal cerebral ischemia. *Brain Stimul*. 2020;13:881–890. doi: 10.1016/j.brs.2020.03.008
29. Konstas AA, Goldmakher GV, Lee TY, Lev MH. Theoretic basis and technical implementations of CT perfusion in acute ischemic stroke, part 2: technical implementations. *AJNR Am J Neuroradiol*. 2009;30:885–892. doi: 10.3174/ajnr.A1492
30. Gleń A, Chrzan R, Urbanik A. The effect of software post-processing applications on identification of the penumbra and core within the ischaemic region in perfusion computed tomography. *Pol J Radiol*. 2019;84:e118–e125. doi: 10.5114/pjr.2019.83182

31. Baron JC. Perfusion thresholds in human cerebral ischemia: historical perspective and therapeutic implications. *Cerebrovasc Dis*. 2001;11(suppl 1):2–8. doi: 10.1159/000049119
32. Kawano H, Bivard A, Lin L, Ma H, Cheng X, Aviv R, O'Brien B, Butcher K, Lou M, Zhang J, et al. Perfusion computed tomography in patients with stroke thrombolysis. *Brain*. 2017;140:684–691. doi: 10.1093/brain/aww338
33. Chen C, Parsons MW, Clapham M, Oldmeadow C, Levi CR, Lin L, Cheng X, Lou M, Kleinig TJ, Butcher KS, et al. Influence of penumbral reperfusion on clinical outcome depends on baseline ischemic core volume. *Stroke*. 2017;48:2739–2745. doi: 10.1161/STROKEAHA.117.018587
34. Faizy TD, Kabiri R, Christensen S, Mlynash M, Kuraitis G, Broocks G, Hanning U, Nawabi J, Lansberg MG, Marks MP, et al. Perfusion imaging-based tissue-level collaterals predict ischemic lesion net water uptake in patients with acute ischemic stroke and large vessel occlusion. *J Cereb Blood Flow Metab*. 2021;41:2067–2075. doi: 10.1177/0271678X21992200
35. Hong G, Antaris AL, Dai H. Near-infrared fluorophores for biomedical imaging. *Nat Biomed Eng*. 2017;1:0010.
36. Yu L, Nguyen E, Liu G, Choi B, Chen Z. Spectral Doppler optical coherence tomography imaging of localized ischemic stroke in a mouse model. *J Biomed Opt*. 2010;15:066006. doi: 10.1117/1.3505016
37. Lee J, Radhakrishnan H, Wu W, Daneshmand A, Climov M, Ayata C, Boas DA. Quantitative imaging of cerebral blood flow velocity and intracellular motility using dynamic light scattering-optical coherence tomography. *J Cereb Blood Flow Metab*. 2013;33:819–825. doi: 10.1038/jcbfm.2013.20
38. Liu YH, Chan SJ, Pan HC, Bandla A, King NKK, Wong PTH, Chen YY, Ng WH, Thakor NV, Liao LD. Integrated treatment modality of cathodal-transcranial direct current stimulation with peripheral sensory stimulation affords neuroprotection in a rat stroke model. *Neurophotonics*. 2017;4:045002. doi: 10.1117/1.NPh.4.4.045002
39. Bornstein NM, Saver JL, Diener HC, Gorelick PB, Shuaib A, Solberg Y, Thackeray L, Savic M, Janelidze T, Zarqua N, et al; ImpACT-24B investigators. An injectable implant to stimulate the sphenopalatine ganglion for treatment of acute ischaemic stroke up to 24 h from onset (ImpACT-24B): an international, randomised, double-blind, sham-controlled, pivotal trial. *Lancet*. 2019;394:219–229. doi: 10.1016/S0140-6736(19)31192-4
40. Hancock AM, Frostig RD. Testing the effects of sensory stimulation as a collateral-based therapeutic for ischemic stroke in c57bl/6j and cd1 mouse strains. *PLoS One*. 2017;12:e0183909. doi: 10.1371/journal.pone.0183909
41. von Bornstädt D, Houben T, Seidel JL, Zheng Y, Dilekoz E, Qin T, Sandow N, Kura S, Eikermann-Haerter K, Endres M, et al. Supply-demand mismatch transients in susceptible peri-infarct hot zones explain the origins of spreading injury depolarizations. *Neuron*. 2015;85:1117–1131. doi: 10.1016/j.neuron.2015.02.007
42. Rakers C, Petzold GC. Astrocytic calcium release mediates peri-infarct depolarizations in a rodent stroke model. *J Clin Invest*. 2017;127:511–516. doi: 10.1172/JCI89354
43. Fordsmann JC, Murmu RP, Cai C, Brazhe A, Thomsen KJ, Zambach SA, Lønstrup M, Lind BL, Lauritzen M. Spontaneous astrocytic Ca2+ activity abounds in electrically suppressed ischemic penumbra of aged mice. *Glia*. 2019;67:37–52. doi: 10.1002/glia.23506